Organometallics 1992, *11*, 3063-3068

Metalation of the Crown Thioether Ligand 2,6,10-Trithia[11]-*m*-cyclophane (TT[11]MC). Synthesis, Structure, and Reactivity of [Pt(TT[11]MC)][BF$_4$] and Structures of [Pt(PPh$_2$Me)(TT[11]MC)][BF$_4$] and [PtI$_2$(TT[11]MC)][BF$_4$]

Garry S. Hanan, James E. Kickham, and Stephen J. Loeb*

Department of Chemistry and Biochemistry, University of Windsor, Windsor, Ontario, Canada N9B 3P4

Received March 18, 1992

The reaction of PtCl$_2$(1,5-COD) with the 1,3-xylyl-containing crown thioether 2,6,10-trithia[11]-*m*-cyclophane (TT[11]MC) in the presence of 1 equiv of AgBF$_4$ yielded [Pt(TT[11]MC)][BF$_4$]. ^{1}H and ^{13}C{^{1}H} NMR spectroscopy indicated that metalation of the ligand at the 2-position of the aromatic ring had occurred, and this was verified by an X-ray crystal structure. The complex [Pt(TT[11]MC)][BF$_4$] crystallized in the space group $P2_1/c$ with $a = 8.373$ (1) Å, $b = 21.784$ (7) Å, $c = 9.517$ (4) Å, $\beta = 95.09$ (2)°, $V = 1729.1$ (16) Å^3, and $Z = 4$. The structure was refined to $R = 6.93\%$ and $R_w = 6.99\%$ for 1885 reflections with $F_o^2 > 3\sigma(F_o^2)$. The Pt atom is in a square-planar environment, bonded to the three S atoms and the aromatic C atom of the macrocycle. In the presence of strong donors such as PPh$_2$Me, [Pt(TT[11]MC)][BF$_4$] undergoes substitution reactions for the S donor trans to the Pt–C bond. The product [Pt(PPh$_2$Me)(TT[11]MC)][BF$_4$] was characterized by ^{1}H, ^{13}C{^{1}H}, and ^{31}P{^{1}H} NMR spectroscopy as well as an X-ray crystal structure. The complex [Pt(PPh$_2$Me)(TT[11]MC)][BF$_4$] crystallized in the space group $P2_1/n$ with $a = 9.933$ (2) Å, $b = 20.163$ (3) Å, $c = 14.490$ (2) Å, $\beta = 94.88$ (2)°, $V = 2891.6$ (16) Å^3, and $Z = 4$. The structure was refined to $R = 5.91\%$ and $R_w = 6.14\%$ for 2841 reflections with $F_o^2 > 3\sigma(F_o^2)$. The Pt atom is in a square-planar environment, bonded to the two mutually trans S atoms, the PPh$_2$Me ligand, and the aromatic C atom of the macrocycle. The remaining S atom is oriented away from the metal center with the aliphatic chain perpendicular to the square plane. [Pt(TT[11]MC)][BF$_4$] also undergoes oxidative-addition reactions with I$_2$ and CuCl$_2$ to produce octahedral Pt(IV) complexes of the type [PtX$_2$(TT[11]MC)][BF$_4$]. These complexes were characterized by ^{1}H and ^{13}C{^{1}H} NMR spectroscopy and an X-ray crystal structure of [PtI$_2$(TT[11]MC)][BF$_4$]. The complex [PtI$_2$(TT[11]MC)][BF$_4$] crystallized in the space group $P2_1/n$ with $a = 11.253$ (4) Å, $b = 11.120$ (2) Å, $c = 16.558$ (4) Å, $\beta = 99.53$ (3)°, $V = 2043$ (2) Å^3, and $Z = 4$. The structure was refined to $R = 6.50\%$ and $R_w = 6.95\%$ for 2464 reflections with $F_o^2 > 3\sigma(F_o^2)$. The Pt atom is in an octahedral environment, comprised of the three S atoms, the xylyl C atom of the macrocycle, and the two added I atoms, which are mutually *cis* in positions *trans* to C and *trans* to the central S atom.

Introduction

A wide variety of crown thioether complexes are known, and the stability and distinct redox properties of these complexes have been partly attributed to the sulfur coordination sphere.[1-4] The functionalization of these thioether macrocycles is of current interest and is certainly one of the next steps in the evolution of their chemistry.[5] Our recent research, employing thiacyclophanes[6] as a class of crown thioether ligand,[7,8] prompted us to investigate the possibility of *ortho* metalation inside the macrocycle as a way of introducing a novel functional group; the M–C σ-bond. A great number of phosphorus and nitrogen donor ligands are known to undergo facile *ortho* metalation;[9] however, work on related thioether systems is quite limited.[10] The majority of the investigations into sulfur-based systems have involved metalation of open-chain ligands such as benzyl thioether derivatives by employing either manganese or palladium. Our approach has been metalation of the aromatic ring contained in thiacyclophanes such as 2,6,10-trithia[11]-*m*-cyclophane (TT[11]MC).[11]

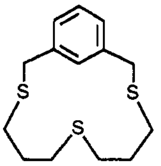

TT[11]MC

The three sulfur atoms of this cyclic ligand can then provide the remaining donors required for square-planar metal coordination. Herein, we describe the synthesis and reaction chemistry of the Pt(II) complex [Pt(TT[11]MC)][BF$_4$], a rare example of a macrocyclic complex

---

[1] Cooper, S. R. *Acc. Chem. Res.* **1988**, *21*, 141–146.

[2] Schröder, M. *Pure Appl. Chem.* **1988**, *60*, 517–524.

[3] Blake, A. J.; Schröder, M. *Adv. Inorg. Chem.* **1990**, *35*, 1–80.

[4] Cooper, S. R.; Rawle, S. C. *Struct. Bonding* **1990**, *72*, 1–72.

[5] (a) Buter, J.; Kellogg, R. M.; van Bolhuis, F. *J. Chem. Soc., Chem. Commun.* **1990**, 282–283. (b) Setzer, W. N.; Cacioppo, E. L.; Guo, Q.; Grant, G. J.; Kim, D. D.; Hubbard, J. L.; Van Derveer, D. G. *Inorg. Chem.* **1990**, *29*, 2672–2681.

[6] Vögtle, F. *Liebigs Ann. Chem.* **1976**, 891.

[7] (a) de Groot, B.; Loeb, S. J. *Inorg. Chem.* **1990**, *29*, 4084–4095. (b) de Groot, B.; Giesbrecht, G. R.; Loeb, S. J.; Shimizu, G. K. H. *Inorg. Chem.* **1991**, *30*, 177–182. (c) de Groot, B.; Hanan, G. S.; Loeb, S. J. *Inorg. Chem.* **1991**, *31*, 4644–4647. (d) Loeb, S. J.; Shimizu, G. K. S. *Can. J. Chem.* **1991**, *69*, 1141–1145.

[8] Loeb, S. J.; Shimizu, G. K. H. *J. Chem. Soc., Chem. Commun.* **1991**, 1119–1121.

[9] (a) Constable, E. C. *Polyhedron* **1984**, *3*, 1037–1057. (b) Omae, I. *Coord. Chem. Rev.* **1979**, *79*, 287–301. (c) Bruce, M. I. *Angew. Chem., Int. Ed. Engl.* **1977**, *16*, 73–86.

[10] (a) Hanton, L. R.; Kemmit, T. *J. Chem. Soc., Chem. Commun.* **1991**, 700–702. (b) Omae, I. *Coord. Chem. Rev.* **1979**, *79*, 97–115.

[11] (a) This ligand was named 2,6,10-trithia[11]-*m*-benzenophane in ref 14 and abbreviated TT[11]MB in accordance with nomenclature originally used for molecules of this type. The term cyclophane used herein is a more correct one. The numeral in brackets indicates the number of atoms in the aliphatic chain in accordance with standard cyclophane nomenclature. (b) Whenever the abbreviation TT[11]MC is used as part of a platinum metal complex, this refers to the formally anionic, metalated species.

0276-7333/92/2311-3063$03.00/0

containing a direct M–C bond.[12] Substitution reactions show the consequences of having all the donor atoms provided by a single macrocyclic ligand and the strong trans influence of the metalated C atom. The oxidative-addition chemistry of this unique complex is also of interest, as it results in ortho-metalated Pt(IV) species, which until recently[13] were relatively scarce. Part of this work has been the subject of a preliminary communication.[14]

Experimental Section

$PtCl_2$(COD) (COD = 1,5-cyclooctadiene)[15] and 2,6,10-trithia-[11]-*m*-cyclophane (TT[11]MC)[16] were prepared by the literature methods. $AgBF_4$, PPh_3, PPh_2Me, dimethyl acetylenedicarboxylate (DMAD), ethylene, CH_3CN, and all deuterated solvents were purchased from Aldrich and used as received. All reactions were conducted under an atmosphere of N_2 using standard Schlenk techniques, and all solvents were degassed prior to use. ^{1}H, ^{13}C{^{1}H}, and ^{31}P{^{1}H} NMR spectra were recorded at 300.1, 75.4, and 121.5 MHz, respectively, on a Bruker AC300 spectrometer locked onto the deuterated solvent. Infrared spectra were recorded on a Nicolet 5DX FT spectrometer. Elemental analyses were performed by Microanalytical Services, New Westminister, British Columbia, Canada.

Preparation of [Pt(TT[11]MC)][BF$_4$]. $PtCl_2$(COD) (0.399 g, 1.07 mmol), TT[11]MC (0.303 g, 1.07 mmol), and $AgBF_4$ (0.216 g, 1.11 mmol) were combined in acetonitrile (100 mL), and the mixture was refluxed for 48 h. The resulting mixture was filtered to remove AgCl and the solvent removed to yield an off-white solid, which was recrystallized from acetonitrile; yield 0.521 (87%). ^{1}H NMR (CD_3CN, 300 K): δ 7.12 (m, 3 H, aromatic), 4.91 (d, 2 H, ^{2}J = 15.9, ^{3}J(Pt) = 70.4 Hz, benzylic), 4.41 (d, ^{2}J = 15.9, benzylic), 3.67 (m, 2 H, ^{3}J(Pt) = 81.1, SCH_2), 3.12–3.33 (m, 4 H, SCH_2), 2.89 (m, 2 H, SCH_2), 2.60 (m, 2 H, CH_2), 2.00 (m, 2 H, CH_2). ^{13}C{^{1}H} NMR: δ 157.9 (^{1}J(Pt) = 854.6 Hz), 147.36 (^{2}J(Pt) = 111.1), 126.57, 122.08 (^{3}J(Pt) $\approx$ 30, aromatic), 52.50 (^{3}J(Pt) $\approx$ 30, benzylic), 38.59 (^{3}J(Pt) = 23.5, SCH_2), 35.75 ($^{3}J \approx$ 20, SCH_2), 28.22 (^{3}J(Pt) = 29.9, CH_2). Anal. Calcd for $C_{14}H_{19}BF_4PtS_3$: C, 29.74; H, 3.39; S, 17.02. Found: C, 29.55; H, 3.26; S, 17.29.

Preparation of [Pt(PPh$_2$Me)(TT[11]MC)][BF$_4$]. [Pt(TT[11]MC)][BF_4] (0.098 g, 0.177 mmol) was dissolved in acetonitrile (15 mL) and PPh_2Me (0.030 mL, 0.177 mmol) added with stirring. The solvent was removed, yielding a colorless solid, which was recrystallized from acetonitrile; yield 0.146 g (85%). ^{1}H NMR (CD_3CN, 300 K) δ 7.67 (m, 4 H, PPh_2Me), 7.53 (m, 6 H, PPh_2Me), 7.17 (m, 3 H, TT[11]MC, aromatic), 4.92 (d, 2 H, ^{2}J = 17.0 Hz, benzylic), 4.43 (d, ^{2}J = 17.0, ^{3}J(Pt) = 37.0, benzylic), 3.14 (m, 2 H, SCH_2), 2.54 (m, 6 H), 2.32 (m, 4 H), 1.77 (br s, 3 H, PMe). ^{13}C{^{1}H} NMR: δ 169.1 (^{1}J(Pt) = 904.8, ^{2}J(P) = 103.3 Hz, TT[11]MC), 150.10 (^{2}J(Pt) = 105.6, TT[11]MC), 133.43 (d, ^{1}J(P) = 48.3, PPh_2Me), 133.45 (^{2}J(P) = 10.6, PPh_2Me), 132.38 (PPh_2Me), 129.97 (^{3}J(P) = 7.5, PPh_2Me), 126.97 (TT[11]MC), 122.21 (TT[11]MC), 52.65 (benzylic), 40.27 (SCH_2), 29.37 (SCH_2), 28.59 (^{3}J(Pt) = 38.1, CH_2), 13.67 (^{1}J(P) = 30.2, PPh_2Me). ^{31}P{^{1}H} NMR: –0.34 (^{1}J(Pt) = 1950.4). Anal. Calcd for $C_{27}H_{32}BF_4PPtS_3$: C, 42.35; H, 4.22; S, 12.66. Found: C, 42.11; H, 4.03; S, 12.69.

Reactions of [Pt(TT[11]MC)][BF$_4$] with CO, H$_2$, and C$_2$H$_4$. [Pt(TT[11]MC)][BF_4] (0.116 g, 2.05 mmol) was dissolved in acetonitrile (25 mL); the solution was placed under 1 atm of CO(g), H_2(g), or C_2H_4(g) and stirred at room temperature for 24 h. The atmosphere was then replaced by N_2(g) and the solvent removed, yielding a colorless solid, which was recrystallized from acetonitrile and identified as [Pt(TT[11]MC)][BF_4] by NMR spectroscopy.

Reactions of [Pt(TT[11]MC)][BF$_4$] with CH$_3$I, PPh$_3$, and DMAD. [Pt(TT[11]MC)][BF_4] (0.116 g, 2.05 mmol) was dissolved in acetonitrile (25 mL) and 1 equiv of the reagent (2.05 mmol) added with stirring. After 24 h, the solvent was removed, yielding a colorless solid, which was recrystallized from acetonitrile and identified as [Pt(TT[11]MC)][BF_4] by NMR spectroscopy.

Preparation of [PtI$_2$(TT[11]MC)][BF$_4$]. [Pt(TT[11]MC)][BF_4] (0.080 g, 1.42 mmol) was dissolved in acetonitrile (20 mL) and I_2 (0.037 g, 0.146 mmol) added with stirring. The mixture was stirred for 12 h and the solvent removed, yielding a dark red solid, which was recrystallized from acetonitrile; yield 0.083 g (71%). ^{1}H NMR (CD_3CN, 300 K): δ 7.27 (m, 2 H), 7.11 (m, 1 H, aromatic), 4.93 (m, 4 H, benzylic), 3.45 (m, 2 H, SCH_2), 3.37 (m, 4 H, SCH_2), 3.10 (m, 2 H, SCH_2), 2.89 (ddd, 2 H, ^{3}J(Pt) = 60.0 Hz, CH_2), 2.41 (m, 2 H, CH_2). ^{13}C{^{1}H} NMR: δ 149.61 (^{1}J(Pt) = 634.0 Hz), 144.79 (^{2}J(Pt) = 51.8), 132.70, 128.40 (^{3}J(Pt) < 30, aromatic), 48.33 (^{3}J(Pt) < 20, benzylic), 34.30 (SCH_2), 32.74 (SCH_2), 21.99 (^{2}J(Pt) = 19.5, CH_2). Anal. Calcd for $C_{14}H_{19}BF_4I_2PtS_3$: C, 20.52; H, 2.34; S, 11.74. Found: C, 20.77; H, 2.43; S, 11.85.

Preparation of [PtCl$_2$(TT[11]MC)][BF$_4$]. [Pt(TT[11]MC)][BF_4] (0.100 g, 0.18 mmol) was dissolved in acetonitrile (20 mL) and $CuCl_2 \cdot 2H_2O$ (0.061 g, 0.35 mmol) added with stirring. Immediately, the solution turned to a pale orange and a yellow solid was deposited. The yellow solid was isolated by filtration, washed with diethyl ether, and dried in vacuo; yield 0.064 g (57%). ^{1}H NMR (DMSO-d_6, 300 K): δ 7.22 (s br, 3 H, aromatic), 4.95 (d br, 4 H, benzylic), 3.35 (m br, 8 H, SCH_2), 2.85 (m br, 4 H, CH_2). ^{13}C{^{1}H} NMR: δ 143.80 (^{1}J(Pt) = 625.0 Hz), 142.87 (^{2}J(Pt) = 43.7), 127.35, 125.34 (aromatic), 44.77 (benzylic), 33.31 (SCH_2), 32.18 (SCH_2), 21.13 (CH_2). Anal. Calcd for $C_{14}H_{19}BCl_2F_4PtS_3$: C, 26.42; H, 3.02; S, 15.12. Found: C, 26.22; H, 3.14; S, 15.21.

General X-ray Diffraction Data Collection, Solution, and Refinement. Diffraction experiments were performed on a four-circle Rigaku AFC6S diffractometer with monochromatized Mo Kα radiation. Cell constants and orientation matrices for data collection were obtained from least-squares refinements using the setting angles of 25 centered reflections. Machine parameters, crystal data, and data collection parameters are summarized in Table I. The intensities of three standard reflections were recorded every 150 reflections and showed no statistically significant changes over the duration of the data collections. Empirical absorption corrections, based on ψ-scan data, were applied to the data. The data were processed by using the TEXSAN software package,[17] running on a VAX 3520 Workstation. Refinements were carried out by using full-matrix least-squares techniques on F, minimizing the function $\sum w(|F_o| - |F_c|)^2$, where $w = 4F_o^2/\sigma^2(F_o^2)$ and F_o and F_c are the observed and calculated structure factors. Atomic scattering factors[18] and anomalous dispersion terms[19,20] were taken from the usual sources. Fixed H atom contributions were included with C–H distances of 0.95 Å and thermal parameters 1.2 times the isotropic thermal parameter of the bonded C atoms. No H atoms were refined, but all values were updated as refinement continued.

Structure Determination of [Pt(TT[11]MC)][BF$_4$]. Colorless crystals of [Pt(TT[11]MC)][BF_4] were grown by vapor diffusion of diethyl ether into an acetonitrile solution of the complex. The position of the platinum atom was determined by conventional Patterson methods. The remaining non-hydrogen atoms were located from difference Fourier map calculations. In the final cycles of refinement, the platinum, sulfur, fluorine, boron, and carbon atoms were all assigned anisotropic thermal parameters. This resulted in $R = \sum||F_o| - |F_c|/\sum|F_o|| = 0.0693$ and $R_w = (\sum w(|F_o| - |F_c|)^2/\sum wF_o^2)^{1/2} = 0.0699$ at final convergence. A goodness-of-fit calculation resulted in a value of 2.17. Selected atomic positional parameters are summarized in Table II, and selected bond distances and angles are summarized in Table III. Nonessential bond distances and angles, thermal parameters, and hydrogen atom parameters are deposited as supplementary material.

---

(12) Terheijden, J.; van Koten, G.; van Beek, J. A. M.; Vriesema, B. K.; Kellogg, R. M.; Zoutberg, M. C.; Stam, C. M. *Organometallics* **1987**, *6*, 89–93.

(13) (a) Chattopadhyay, S.; Sinha, C.; Basu, P.; Chakravorty, A. *Organometallics* **1991**, *10*, 1135–1139 and references therein.

(14) Hanan, G. S.; Kickham, J. E.; Loeb, S. J. *J. Chem. Soc., Chem. Commun.* **1991**, 893–895.

(15) Clark, H. C.; Manzer, L. E. *J. Organomet. Chem.* **1973**, *59*, 411.

(16) Giesbrecht, G. R.; Hanan, G. S.; Kickham, J. E.; Loeb, S. J. *Inorg. Chem.*, in press.

(17) TEXSAN-TEXRAY Structure Analysis Package, Molecular Structure Corp., 1985.

(18) Cromer, D. T.; Waber, J. T. *International Tables for X-ray Crystallography*; Kynoch Press: Birmingham, United Kingdom, 1974; Vol. IV, Table 2.2A.

(19) Ibers, J. A.; Hamilton, W. C. *Acta Crystallogr., Sect. A* **1974**, *17*, 781.

(20) Cromer, D. T. *International Tables for X-ray Crystallography*; Kynoch Press: Birmingham, United Kingdom, 1974; Vol. IV, Table 2.3.1.

Table I. Summary of Crystal Data, Intensity Collection, and Structure Refinement for [Pt(TT[11]MC)][BF_4], [Pt(PPh_2Me)(TT[11]MC)][BF_4], and [PtI_2(TT[11]MC)][BF_4]

chem formula	$C_{14}H_{19}BF_4PtS_3$	$C_{27}H_{32}BF_4PPtS_3$	$C_{14}H_{19}BF_4I_2PtS_3$
cryst color, form	colorless prism	colorless prism	deep red prism
fw	565.38	765.65	819.19
a, Å	8.373 (1)	9.933 (2)	11.253 (4)
b, Å	21.784 (7)	20.163 (3)	11.120 (2)
c, Å	9.517 (4)	14.490 (2)	16.558 (4)
β, deg	95.09 (2)	94.88 (2)	99.53 (3)
cryst syst	monoclinic	monoclinic	monoclinic
space group	$P2_1/c$ (No. 14)	$P2_1/n$ (No. 14)	$P2_1/n$ (No. 14)
V, Å^3	1729.1 (16)	2891.6 (16)	2043 (2)
ρ(calcd), g cm^{-3}	2.172	1.795	2.662
Z	4	4	4
cryst dimens, mm	0.36 × 0.21 × 0.37	0.21 × 0.15 × 0.20	0.12 × 0.28 × 0.33
μ, cm^{-1}	85.79 (empirical)	52.10 (empirical)	102.56 (empirical)
diffractometer	Rigaku AFC6	Rigaku AFC6	Rigaku AFC6
λ, Å	0.71069	0.71069	0.71069
T, °C	24	24	24
takeoff angle, deg	6.0	6.0	6.0
aperature, mm	6.0 horiz, 6.0 vert	6.0 horiz, 6.0 vert	6.0 horiz, 6.0 vert
cryst/det dist, cm	40	40	40
scan type	ω–2θ	ω–2θ	ω–2θ
speed, deg min^{-1}	32.0	32.0	32.0
width, deg	1.05 + 0.30 tan θ	1.05 + 0.30 tan θ	1.05 + 0.30 tan θ
no. of data collected	3139	5572	3803
no. of unique data with $F_o^2 > 3\sigma(F_o^2)$	1885	2841	2464
no. of variables	209	344	227
goodness of fit	2.172	1.687	2.124
$R(F_o)$, %	6.93	5.91	6.50
$R_w(F_o)$, %	6.99	6.14	6.95

Table II. Positional Parameters and *B*(eq) Values for [Pt(TT[11]MC)][BF_4]

atom	*x*	*y*	*z*	*B*(eq), Å^2
Pt	0.10588 (9)	0.10848 (4)	0.10585 (9)	2.51 (4)
S1	−0.0437 (6)	0.0366 (3)	0.2033 (7)	3.8 (3)
S2	0.3229 (6)	0.0451 (3)	0.0554 (6)	2.9 (2)
S3	0.1867 (6)	0.1893 (3)	−0.0199 (6)	3.1 (3)
C1	−0.054 (2)	0.165 (2)	0.177 (2)	5 (1)
C2	−0.049 (3)	0.230 (1)	0.143 (2)	4 (1)
C3	−0.163 (3)	0.267 (1)	0.189 (3)	4 (1)
C4	−0.273 (2)	0.248 (1)	0.275 (3)	5 (1)
C5	−0.268 (2)	0.188 (1)	0.322 (2)	4 (1)
C6	−0.156 (2)	0.146 (1)	0.274 (3)	4 (1)
C7	−0.133 (2)	0.084 (1)	0.332 (2)	4 (1)
C8	0.079 (3)	−0.018 (1)	0.307 (3)	4 (1)
C9	0.204 (3)	−0.047 (1)	0.228 (3)	6 (1)
C10	0.348 (3)	−0.0076 (12)	0.208 (3)	4 (1)
C11	0.490 (2)	0.0951 (10)	0.109 (2)	3.0 (6)
C12	0.500 (2)	0.1510 (10)	0.013 (2)	3 (1)
C13	0.392 (2)	0.2053 (11)	0.045 (2)	4 (1)
C14	0.077 (3)	0.252 (1)	0.056 (3)	5 (1)
F1	0.415 (3)	0.1455 (10)	0.659 (2)	12 (2)
F2	0.314 (3)	0.1411 (12)	0.437 (2)	13 (2)
F3	0.502 (3)	0.0867 (11)	0.512 (3)	11 (2)
F4	0.266 (4)	0.073 (2)	0.579 (4)	22 (3)
B	0.360 (4)	0.106 (2)	0.558 (5)	7 (2)

Table III. Selected Bond Distances and Angles for [Pt(TT[11]MC)][BF_4]

	Distances (Å)		
Pt–S1	2.255 (6)	C1–C6	1.38 (3)
Pt–S2	2.365 (5)	C2–C3	1.35 (3)
Pt–S3	2.266 (6)	C2–C14	1.48 (3)
Pt–C1	1.99 (3)	C3–C4	1.35 (3)
S1–C7	1.81 (3)	C4–C5	1.37 (4)
S1–C8	1.81 (3)	C5–C6	1.41 (3)
S2–C10	1.85 (3)	C6–C7	1.47 (3)
S2–C11	1.81 (3)	C8–C9	1.48 (4)
S3–C13	1.81 (3)	C9–C10	1.50 (3)
S3–C14	1.83 (3)	C11–C12	1.53 (3)
C1–C2	1.44 (4)	C12–C13	1.54 (3)
	Angles (deg)		
S1–Pt–S2	98.2 (2)	C3–C4–C5	119 (2)
S1–Pt–S3	163.6 (2)	C4–C5–C6	121 (2)
S2–Pt–S3	94.3 (2)	C5–C6–C1	119 (3)
S1–Pt–C1	83.0 (9)	C5–C6–C7	123 (2)
S2–Pt–C1	170.4 (6)	C6–C7–S1	109 (2)
S3–Pt–C1	86.4 (9)	S1–C8–C9	113 (2)
C7–S1–C8	105 (1)	C8–C9–C10	116 (3)
C10–S2–C11	97 (1)	C9–C10–S2	114 (2)
C13–S3–C14	103 (1)	S2–C11–C12	113 (1)
C2–C1–C6	118 (2)	C12–C13–S3	110 (2)
C1–C2–C3	118 (2)	S3–C14–C2	112 (2)
C1–C2–C14	119 (2)	C2–C3–C4	123 (4)

Structure Determination of [Pt(PPh_2Me)(TT[11]MC)][BF_4]. Colorless crystals of [Pt(PPh_2Me)(TT[11]MC)][BF_4] were grown by slow evaporation of an acetonitrile solution of the complex. The position of the platinum atom was determined by the Patterson method, and the remaining non-hydrogen atoms were located from difference Fourier map calculations. In the final cycles of refinement, the platinum, sulfur, phosphorus, fluorine, boron, and carbon atoms were all assigned anisotropic thermal parameters. This resulted in $R = 0.0591$ and $R_w = 0.0614$ at final convergence. A goodness-of-fit calculation resulted in a value of 1.69. Selected atomic positional parameters are summarized in Table IV, and selected bond distances and angles are summarized in Table V. Nonessential bond distances and angles, thermal parameters, and hydrogen atom parameters are deposited as supplementary material.

Structure Determination of [PtI_2(TT[11]MC)][BF_4]. Dark red crystals of [PtI_2(TT[11]MC)][BF_4] were grown by slow evaporation of an acetonitrile solution of the complex. The positions of the platinum atom and the iodine atoms were determined by direct methods from the *E*-map with highest figure of merit. The remaining non-hydrogen atoms were located from difference Fourier map calculations. In the final cycles of refinement, the platinum, iodine, sulfur, fluorine, boron, and carbon atoms were all assigned anisotropic thermal parameters. This resulted in $R = 0.0650$ and $R_w = 0.0695$ at final convergence. A goodness-of-fit calculation resulted in a value of 2.12. Selected atomic positional parameters are summarized in Table VI, and selected bond distances and angles are summarized in Table VII. Nonessential bond distances and angles, thermal parameters, and hydrogen atom parameters are deposited as supplementary material.

Results and Discussion

Metalation of TT[11]MC by Platinum(II). The reaction of equimolar amounts of TT[11]MC and $PtCl_2$(1,5-COD) in the presence of 1 equiv of $AgBF_4$, in refluxing

Table IV. Positional Parameters and B(eq) Values for $[Pt(PPh_2Me)(TT[11]MC)][BF_4]$

atom	x	y	z	B(eq), Å^2
Pt	0.01548 (7)	0.17887 (3)	0.05299 (9)	2.34 (3)
S1	0.0301 (4)	0.0886 (2)	0.1493 (3)	2.8 (2)
S2	−0.1537 (5)	0.2925 (2)	0.2857 (3)	3.8 (2)
S3	0.0409 (5)	0.2738 (2)	−0.0307 (3)	3.2 (2)
P1	−0.1843 (5)	0.1470 (2)	−0.0334 (2)	2.9 (2)
C1	0.197 (2)	0.2011 (8)	0.1133 (12)	3.0 (8)
C2	0.275 (2)	0.2540 (9)	0.084 (1)	3 (1)
C3	0.403 (2)	0.2673 (8)	0.126 (1)	4 (1)
C4	0.458 (2)	0.2328 (10)	0.200 (1)	4 (1)
C5	0.368 (2)	0.1790 (10)	0.2295 (12)	3.7 (9)
C6	0.257 (2)	0.1642 (8)	0.1907 (12)	2.9 (8)
C7	0.183 (2)	0.1066 (10)	0.223 (1)	4 (1)
C8	−0.101 (2)	0.0925 (8)	0.2307 (12)	2.8 (8)
C9	−0.166 (2)	0.1587 (8)	0.2465 (12)	2.9 (8)
C10	−0.072 (2)	0.2122 (8)	0.2856 (10)	2.7 (8)
C11	−0.163 (2)	0.3108 (8)	0.163 (1)	3.6 (9)
C12	−0.041 (2)	0.3419 (8)	0.129 (1)	3.5 (9)
C13	−0.043 (2)	0.3419 (8)	0.025 (1)	4 (1)
C14	0.216 (2)	0.2929 (10)	0.003 (1)	4 (1)
C15	−0.149 (2)	0.1152 (8)	−0.1469 (12)	2.9 (8)
C16	−0.015 (2)	0.1080 (7)	−0.168 (1)	3.1 (8)
C17	0.014 (2)	0.0803 (9)	−0.253 (1)	4 (1)
C18	−0.094 (3)	0.0607 (8)	−0.312 (1)	4 (1)
C19	−0.224 (2)	0.0661 (10)	−0.291 (1)	5 (1)
C20	−0.251 (2)	0.0932 (9)	−0.209 (1)	3.3 (9)
C21	−0.277 (2)	0.0801 (8)	0.015 (1)	3.3 (9)
C22	−0.232 (2)	0.0161 (8)	0.011 (1)	3.1 (8)
C23	−0.291 (2)	−0.0362 (9)	0.054 (1)	4 (1)
C24	−0.396 (2)	−0.021 (1)	0.111 (1)	5 (1)
C25	−0.439 (2)	0.0425 (12)	0.117 (2)	5 (1)
C26	−0.385 (2)	0.0941 (9)	0.071 (1)	4 (1)
C27	−0.309 (2)	0.2123 (8)	−0.062 (1)	4 (1)
F1	0.838 (2)	0.0530 (9)	0.4392 (11)	11 (1)
F2	0.628 (2)	0.0619 (11)	0.380 (2)	14 (2)
F3	0.735 (2)	−0.0263 (8)	0.362 (1)	14 (1)
F4	0.678 (2)	−0.0031 (11)	0.4987 (12)	13 (1)
B	0.721 (3)	0.019 (2)	0.421 (2)	6 (2)

Table V. Selected Bond Distances and Angles for $[Pt(PPh_2Me)(TT[11]MC)][BF_4]$

Distances (Å)			
Pt–S1	2.290 (4)	C1–C6	1.43 (2)
Pt–S3	2.292 (5)	C2–C3	1.39 (2)
Pt–P1	2.344 (5)	C2–C14	1.49 (2)
Pt–C1	1.99 (2)	C3–C4	1.35 (3)
S1–C7	1.82 (2)	C4–C5	1.39 (2)
S1–C8	1.83 (2)	C5–C6	1.39 (2)
S2–C10	1.81 (2)	C6–C7	1.47 (2)
S2–C11	1.81 (2)	C8–C9	1.51 (2)
S3–C13	1.83 (2)	C9–C10	1.50 (2)
S3–C14	1.81 (2)	C11–C12	1.48 (2)
C1–C2	1.40 (2)	C12–C13	1.51 (2)
P1–C15	1.83 (2)	P1–C21	1.81 (2)
P1–C27	1.83 (2)		
Angles (deg)			
S1–Pt–S3	169.1 (3)	C3–C4–C5	117 (2)
S1–Pt–P1	96.6 (2)	C4–C5–C6	122 (2)
S3–Pt–P1	94.2 (2)	C5–C6–C1	121 (2)
S1–Pt–C1	84.4 (5)	C5–C6–C7	121 (2)
S3–Pt–C1	84.7 (5)	C6–C7–S1	113 (2)
P1–Pt–C1	172.7 (5)	S1–C8–C9	118 (1)
C7–S1–C8	102.7 (9)	C8–C9–C10	116 (1)
C10–S2–C11	99.5 (7)	C9–C10–S2	112 (1)
C13–S3–C14	100.7 (9)	S2–C11–C12	116 (1)
C2–C1–C6	116 (2)	C12–C13–S3	118 (1)
C1–C2–C3	121 (2)	S3–C14–C2	114 (1)
C1–C2–C14	117 (2)	C2–C3–C4	123 (2)

acetonitrile, yields $[Pt(TT[11]MC)][BF_4]$ as a colorless crystalline solid:

$$PtCl_2(COD) + TT[11]MC \xrightarrow[CH_3CN]{AgBF_4} [Pt(TT[11]MC)][BF_4] + AgCl + HCl + COD$$

Table VI. Positional Parameters and B(eq) Values for $[PtI_2(TT[11]MC)][BF_4]$

atom	x	y	z	B(eq), Å^2
Pt	0.03302 (7)	0.24150 (7)	0.79554 (4)	1.77 (3)
I1	−0.0256 (1)	0.4370 (1)	0.69625 (9)	3.13 (6)
I2	0.0342 (1)	0.3761 (1)	0.92997 (9)	3.27 (7)
S1	0.2365 (5)	0.2909 (5)	0.8155 (3)	3.7 (2)
S2	0.0288 (5)	0.1052 (5)	0.6869 (3)	2.3 (2)
S3	−0.1612 (4)	0.1816 (5)	0.8092 (3)	2.5 (2)
C1	0.084 (2)	0.096 (2)	0.8681 (10)	2.0 (8)
C2	−0.002 (2)	0.009 (2)	0.8769 (11)	3 (1)
C3	0.035 (2)	−0.091 (2)	0.926 (1)	3 (1)
C4	0.155 (2)	−0.103 (5)	0.961 (1)	4 (1)
C5	0.238 (2)	−0.020 (2)	0.9480 (12)	3 (1)
C6	0.203 (2)	0.083 (2)	0.900 (1)	3 (1)
C7	0.294 (2)	0.178 (2)	0.890 (1)	4 (1)
C8	0.304 (2)	0.259 (2)	0.725 (1)	3 (1)
C9	0.266 (2)	0.144 (3)	0.680 (1)	4 (1)
C10	0.142 (2)	0.147 (2)	0.6269 (12)	3 (1)
C11	−0.106 (2)	0.133 (2)	0.6128 (12)	3 (1)
C12	−0.223 (2)	0.103 (2)	0.643 (1)	4 (1)
C13	−0.259 (2)	0.179 (2)	0.709 (1)	3 (1)
C14	−0.127 (2)	0.021 (2)	0.835 (1)	3 (1)
F1	0.9916 (11)	0.1266 (11)	0.4278 (7)	3.8 (6)
F2	1.1935 (10)	0.140 (1)	0.4480 (8)	4.2 (6)
F3	1.083 (1)	0.186 (2)	0.3242 (8)	5.8 (8)
F4	1.081 (1)	0.310 (1)	0.4329 (10)	6.6 (8)
B	1.089 (3)	0.193 (2)	0.409 (2)	3 (1)

Table VII. Selected Bond Distances and Angles for $[PtI_2(TT[11]MC)][BF_4]$

Distances (Å)			
Pt–I1	2.739 (2)	C1–C2	1.39 (3)
Pt–I2	2.681 (2)	C1–C6	1.37 (3)
Pt–S1	2.325 (5)	C2–C3	1.39 (3)
Pt–S2	2.346 (5)	C2–C14	1.47 (3)
Pt–S3	2.331 (5)	C3–C4	1.39 (3)
Pt–C1	2.04 (2)	C4–C5	1.36 (3)
S1–C7	1.81 (2)	C5–C6	1.41 (3)
S1–C8	1.82 (2)	C6–C7	1.50 (3)
S2–C10	1.80 (2)	C8–C9	1.51 (3)
S2–C11	1.81 (2)	C9–C10	1.53 (3)
S3–C13	1.83 (2)	C11–C12	1.52 (3)
S3–C14	1.86 (2)	C12–C13	1.49 (3)
Angles (deg)			
I1–Pt–I2	91.31 (5)	C7–S1–C8	106 (1)
I1–Pt–S1	91.8 (1)	C10–S2–C11	99.7 (9)
I1–Pt–S2	94.6 (1)	C13–S3–C14	105 (1)
I1–Pt–S3	98.5 (1)	C2–C1–C6	123 (2)
I1–Pt–C1	177.6 (5)	C1–C2–C3	118 (2)
I2–Pt–S1	83.1 (1)	C1–C2–C14	121 (2)
I2–Pt–S2	173.7 (1)	C2–C3–C4	120 (2)
I2–Pt–S3	87.4 (1)	C3–C4–C5	121 (2)
I2–Pt–C1	89.6 (5)	C4–C5–C6	120 (2)
S1–Pt–S2	99.0 (2)	C5–C6–C7	120 (2)
S1–Pt–S3	166.2 (2)	C5–C6–C1	118 (2)
S1–Pt–C1	86.1 (6)	C6–C7–S1	113 (2)
S2–Pt–S3	89.4 (2)	S1–C8–C9	117 (2)
S2–Pt–C1	84.6 (5)	C8–C9–C10	115 (2)
S3–Pt–C1	83.8 (6)	C9–C10–S2	110 (1)
Pt–C1–C2	119 (2)	S2–C11–C12	114 (1)
Pt–C1–C6	118 (2)	C11–C12–C13	118 (2)
C12–C13–S3	119 (1)	S3–C14–C2	110 (1)

^{1}H and ^{13}C{^{1}H} NMR spectroscopy are consistent with the formulation of this product as a symmetrical complex in which metalation of the aromatic ring of TT[11]MC has occurred. In the ^{1}H NMR spectrum, the absence of a ligand proton resonance at δ 7.43 ppm[16] and splitting of the benzylic resonance into a pair of doublets, with a large three-bond ^{195}Pt coupling of 70.4 Hz to the downfield signal, indicate that metalation has occurred. In addition, the presence of large one- and two-bond ^{195}Pt couplings of 854.6 and 111.1 Hz to downfield-shifted ^{13}C{^{1}H} resonances at δ 157.90 and 147.36 ppm (these resonances occur at δ 128.75 and 139.49 ppm in the free ligand) are evidence

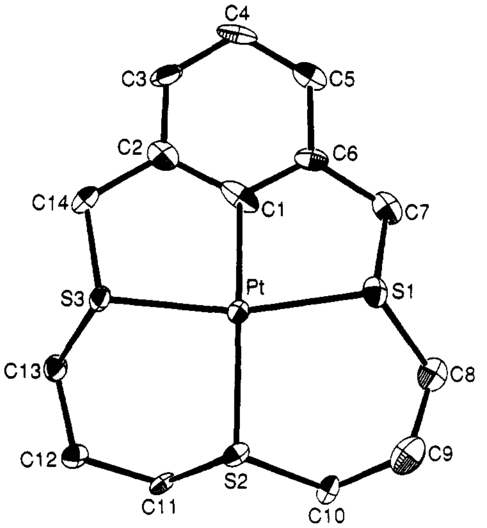

Figure 1. Perspective ORTEP drawing of the $[Pt(TT[11]MC)]^+$ cation showing the atom-numbering scheme.

for the formation of a Pt–C bond at the 2-position of the aromatic ring.

The X-ray structure of $[Pt(TT[11]MC)][BF_4]$ verifies that the Pt atom is in a square-planar PtS_3C environment provided by the metalated macrocycle (Figure 1). The Pt–S distances to the mutually trans S atoms are Pt–S1 = 2.255 (6) Å and Pt–S3 = 2.266 (4) Å, but the Pt–S2 distance trans to the Pt–C1 bond is significantly longer (2.365 (6) Å) due to the strong trans influence of the aromatic group. The Pt–C1 distance is 1.99 (3) Å. The ligand bite angles at the Pt center are S1–Pt–C1 = 83.0 (9)° and S3–Pt–C1 = 86.4 (9)° for the rigid metalated fragment containing the strained five-membered chelate rings and S1–Pt–S2 = 98.2 (2)° and S2–Pt–S3 = 94.3 (2)° for the more flexible six-membered chelate rings. The effect of constraining the Pt(II) center inside the macrocycle is evident from a number of bonding parameters. First, the mutually *trans* Pt–S distances are significantly shorter than those recently found for a series of Pt(II) complexes with open-chain thioether ligands, $[PtX(RS(CH_2)_3S(CH_2)_3SR)]^+$ (X = halide, R = Et, Ph, *i*Pr).[21] The Pt–S bond distances in these complexes ranged from 2.290 (4) to 2.308 (5) Å when no macrocyclic or chelate strain was present. Also, there is a significant tetrahedral distortion at Pt evidenced by the C1–Pt–S2 and S1–Pt–S3 angles of 170.4 (6) and 163.6 (2)°. This distortion presumably arises from the angular constraints of the rigid S–C(aryl)–S portion of the ligand.

Substitution Reactions. Although the Pt(II) center is contained in a macrocycle with a relatively rigid $-SCH_2(C_6H_4)CH_2S-$ fragment, a pathway for substitution chemistry may be available via labilization of the Pt–S2 bond and the flexibility of the $-SCH_2CH_2CH_2SCH_2CH_2CH_2S-$ linkage. Simple substitution reactions were attempted with two-electron-donor molecules. With CO, C_2H_4, and RCCR (R = Ph, COOMe), no reaction could be detected by ^1H NMR spectroscopy, while with stronger donors such as PPh_3 and PPh_2Me, competition for the Pt–S2 site was evident in solution. The results of these reactions indicate that formation of adducts of the type $[Pt(Y)[TT[11]MC)]^+$ are possible, but only strong donors such as Y = PPh_2Me could successfully compete with S2 for the coordination site. A comparison of the $^{13}C\{^1H\}$ NMR chemical shifts for the $-SCH_2CH_2CH_2SCH_2CH_2CH_2S-$ chain atoms of $[Pt(TT[11]MC)][BF_4]$ and $[Pt(PPh_2Me)(TT[11]MC)][BF_4]$ (δ 38.59, 35.75, and 28.22 versus 40.27, 29.37, and 28.59, respectively) are consistent with a conformational change having occurred upon the addition of PPh_2Me. This evidence, combined with the fact that the $^{31}P\{^1H\}$ NMR spectrum shows a single resonance (δ −0.34) with a large ^{195}Pt coupling (1950.4 Hz), suggests that the phosphine ligand substitutes for S2, resulting in a square-planar complex in which the central S2 atom is exodentate and the aliphatic chain is folded away, perpendicular to the PtS_2P plane.

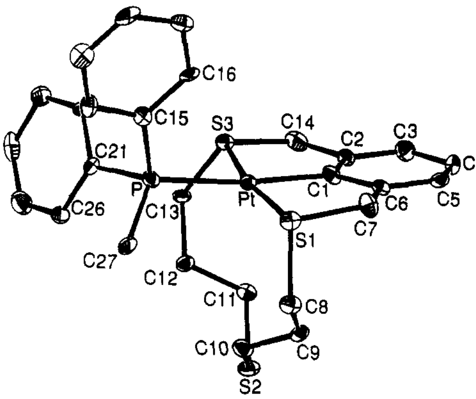

Figure 2. Perspective ORTEP drawing of the $[Pt(PPh_2Me)(TT[11]MC)]^+$ cation showing the atom-numbering scheme.

The X-ray structure of $[Pt(PPh_2Me)(TT[11]MC)][BF_4]$ shows that the Pt atom is indeed in a square-planar PtS_2P environment with the central S donor oriented away from the metal center (Figure 2), as proposed from NMR spectral data. The Pt–S distances to the mutually *trans* S atoms are Pt–S1 = 2.290 (4) Å and Pt–S3 = 2.292 (4) Å, and the Pt–C1 distance is 1.99 (2) Å. The fourth site is occupied by the PPh_2Me ligand with a Pt–P1 distance of 2.344 (5) Å. The angles at the Pt center are S1–Pt–C1 = 84.4 (5)° and S3–Pt–C1 = 84.7 (5)° for the five-membered chelate rings in the metalated portion of the macrocycle and S1–Pt–P1 = 96.6 (2)° and S3–Pt–P1 = 94.2 (2)° to the PPh_2Me ligand. Since the Pt atom is no longer constrained entirely inside the macrocycle, there is much less tetrahedral distortion, as shown by the C1–Pt–P1 and S1–Pt–S3 angles of 172.7 (5)° and 169.1 (3)°. This relaxation of the macrocyclic constraints is also evident in significantly longer Pt–S distances and slightly larger S–Pt–C angles as compared to those in $[Pt(TT[11]MC)][BF_4]$.

Oxidative-Addition Reactions. The apparent lability of the Pt–S2 bond in $[Pt(TT[11]MC)][BF_4]$ and the demonstrated flexibility of TT[11]MC suggests that $[Pt(TT[11]MC)]^+$ might also accommodate the necessary structural changes required for oxidative addition to complexes of Pt(IV) with either *cis* or *trans* addition geometry. The reactions of $[Pt(TT[11]MC)][BF_4]$ with 1 equivalent of either $CuCl_2$ or I_2 yielded the Pt(IV) oxidative-addition products $[PtX_2(TT[11]MC)][BF_4]$, where X = Cl, I; however, no reaction was detected with CH_3I. NMR spectral data for these oxidative-addition products show evidence for the Pt(II) to Pt(IV) oxidation-state change. This is exemplified by the chemical shift and coupling constant for the metalated carbon atom, which are altered dramatically upon oxidation. Thus, for $[Pt(TT[11]MC)][BF_4]$ and $[PtI_2(TT[11]MC)][BF_4]$ the observed data show a downfield shift from δ 157.90 to 149.61 (I) and 143.80 ppm (Cl) and a reduction in the value of $^1J(Pt)$ from 854.6 Hz to 634.0 (I) and 625.0 Hz (Cl). This is a well-established trend and can be attributed to less electron density on the Pt(IV) center as compared to Pt(II).[22]

---

[21] Mansfield, J. R. M.Sc. Thesis, University of Manitoba, 1990.

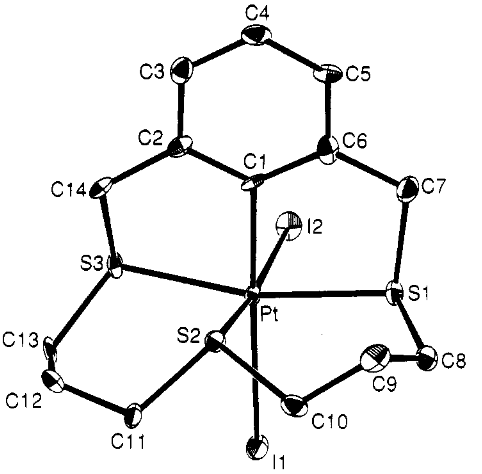

Figure 3. Perspective ORTEP drawing of the $[PtI_2(TT[11]MC)]^+$ cation showing the atom-numbering scheme.

The actual geometry of the Pt(IV) products was determined from the X-ray structure of $[PtI_2(TT[11]MC)][BF_4]$. The structural results show (Figure 3) that addition of I_2 to Pt has occurred to produce an octahedral Pt(IV) species with a PtI_2S_3C coordination sphere in which the I atoms are mutually cis and TT[11]MC is folded such that S2 is coordinated perpendicular to the $PtIS_2C$ plane. The Pt–S distances to the mutually *trans* S atoms are Pt–S1 = 2.325 (5) Å and Pt–S3 = 2.331 (5) Å, and the Pt–S2 distance *trans* to I2 is 2.346 (5) Å. The Pt–I distances are Pt–I1 = 2.739 (2) Å and Pt–I2 = 2.681 (2) Å, with the former reflecting the *trans* influence of the aromatic group, similar to that observed for S2 in $[Pt(TT[11]MC)]^+$. The Pt–C1 distance of 2.04 (2) Å is significantly longer than that found in the structure of $[Pt(TT[11]MC)][BF_4]$ and can be attributed to the higher oxidation state at the metal, the change in coordination geometry, and the presence of extra donors in the six-coordinate complex. The chelate angles associated with the folded macrocycle are S1–Pt–C1 = 86.1 (6)°, S3–Pt–C1 = 83.8 (6)°, and S2–Pt–C1 = 84.6 (5)°, and the Pt center displays a distorted-octahedral geometry as shown by the *trans* angles I1–Pt–C1 = 177.6 (5)°, I2–Pt–S2 = 173.7 (1)°, and S1–Pt–S3 = 166.2 (2)°.

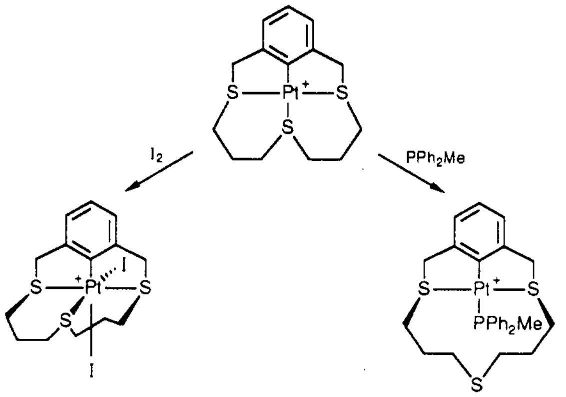

The only example of *ortho* metalation at platinum involving a cyclic ligand is the complex *trans*-[2,6-(2,13-dimethyl-2,13-diazatetradecanediyl)phenyl-*N*,*N*′]platinum(II) iodide, reported by van Koten.[12] In this complex, the ligand is actually a rigid tridentate unit containing a long and flexible $-(CH_2)_{10}-$ chain which simply serves to link the two sides of a metalated 1,3-xylylenediamine fragment without providing further donors. This complex has structural similarities with $[Pt(PPh_2Me)(TT[11]MC)][BF_4]$ in that the aliphatic chain must fold away from the metal coordination site. The difference, however, is that this methylene chain can only effect chemical reactions in a steric or regiospecific manner since it contains no donor atoms. In addition to van Koten's cyclic system, there are a number of open-chain ligand systems of the type $XCH_2C_6H_4CH_2X$ in which X = $N(Me)_2$,[23] SMe,[24] and $P(tBu)_2$.[25] These systems have incorporated metalation of the central aromatic ring carbon, and each displays some interesting chemistry related to the unique X_2C donor set. In particular, the metalated ligand containing $N(Me)_2$ donors has been shown to form stable complexes with Ni(II), Pd(II), Pt(II), and Sn(IV). Several of these complexes have shown unique properties such as a stable Ni^{III}–C σ-bond, a stable R_3Sn^+ cation, and reactivity with small molecules.[23] The incorporation of this type of framework into a thioether macrocycle also has great potential for reaction chemistry, as demonstrated by $[Pt(TT[11]MC)][BF_4]$. The substitution and oxidative-addition reactions outlined herein, for $[Pt(TT[11]MC)][BF_4]$, can be thought of as models for essential reaction pathways required in catalytic chemistry. For a square-planar, 16-electron complex to participate in a catalytic cycle there must be reaction pathways that allow for a single site dissociation and substrate binding as well as *cis* oxidative addition and reductive elimination.[26] The formation of $[Pt(PPh_2Me)(TT[11]MC)][BF_4]$ and $[PtI_2(TT[11]MC)][BF_4]$ from $[Pt(TT[11]MC)][BF_4]$ demonstrates that metalated complexes of TT[11]MC can accommodate these pathways. Complexes of TT[11]MC with more active metals such as Rh(I), Ru(II), and Ir(I) have the potential for exhibiting catalytic chemistry employing a metalated thioether macrocycle, and this possibility is being investigated.

Acknowledgment. We thank the Natural Sciences and Engineering Research Council of Canada for financial support of this research, and G.S.H. is grateful for the awarding of an NSERC undergraduate research scholarship.

Supplementary Material Available: Tables of thermal parameters, nonessential bond distances and angles, and hydrogen atom parameters for $[Pt(TT[11]MC)][BF_4]$, $[Pt(PPh_2Me)(TT[11]MC)][BF_4]$, and $[PtI_2(TT[11]MC)][BF_4]$ (9 pages). Ordering information is given on any current masthead page.

OM920143X

---

(22) Günther, H. *NMR Spectroscopy*; Wiley: New York, 1985.

(23) (a) van Koten, G.; Terheijden, J.; van Beek, J. A. M.; Wehman-Ooyevaar, I. C. M.; Muller, F.; Stam, C. M. *Organometallics* **1990**, *9*, 903 and references cited therein. (b) van Koten, G. *Pure Appl. Chem.* **1989**, *61*, 1681 and references cited therein.

(24) Dupont, J.; Pfeffer, M. *J. Chem. Soc., Dalton Trans.* **1990**, 3193 and references cited therein.

(25) (a) Jouaiti, A.; Geoffroy, M.; Terron, G.; Bernardinelli, G. *J. Chem. Soc., Chem. Commun.* **1992**, 155–156. (b) Moulton, C. J.; Shaw, B. L. *J. Chem. Soc., Dalton Trans.* **1976**, 1020 and references cited therein.

(26) Collman, J. P.; Hegedus, L. S.; Norton, J. R.; Finke, R. J. *Principles and Applications of Organotransition Metal Chemistry*; University Science Books: Mill Valley, CA, 1987.